

Fig. 5. Differential phase shift as a function of frequency for  $a = 1$  cm,  $c - b = 1$  mm,  $\epsilon_r = 15$ ,  $K = 2 \times 10^6/f$

## V. CONCLUSION

A general technique to study propagation in loaded circular cylindrical guiding structures was developed and applied to a cylindrical waveguide containing a coaxial tube of ferrite azimuthally magnetized to remanence (no accurate solution was previously available for this structure). This geometry can be used to realize latching rotators and phase-dependent phase shifters for cross-polarization compensation in high-frequency telecommunications.

Computer results were presented for one particular structure showing the influence of geometric parameters, material properties, and frequency. Since a large number of parameters are involved, it is not possible to present a more general description. It is hoped that the results presented will give a general idea of the behavior of the structure considered. The presence of a thin latching conductor at the waveguide center produces a negligible effect on the propagation constant of the  $HE_{11}$  modes. On the other hand, precautions must be taken not to launch coaxial-line modes over the loaded section. The side connections of the conductor are equivalent to shunt capacitors for one of the linearly polarized modes. Their effect can, however, be compensated over a broad frequency band by the addition of a series inductance at the same location [17]. Device optimization should take into account specified frequency bands and parameters of ferrite materials actually available in tube form. The authors would be pleased to provide, on a complimentary basis, copies of the computer listing to readers interested in pursuing further the study presented here.

## REFERENCES

- [1] A. G. Fox, S. E. Miller, and M. T. Weiss, "Behavior and applications of ferrites in the microwave region," *Bell Syst. Tech. J.*, pp. 5-103, Jan. 1955.
- [2] P. J. B. Claricoats, *Microwave Ferrites*. Chapman and Hall, 1961, pp. 143-146.
- [3] H. Suhl and L. R. Walker, "Topics in guided wave propagation through gyromagnetic media. Part II—Transverse magnetization and the non-reciprocal helix," *Bell Syst. Tech. J.*, pp. 939-986, July 1954.
- [4] N. Kumagai and K. Takeuchi, "Circular electric waves propagating through the circular waveguide containing a circumferentially magnetized ferrite cylinder," *IRE Wescon Convention Record*, pt. I, pp. 123-130, 1958.
- [5] D. M. Bolle and G. S. Heller, "Theoretical considerations on the use of circularly symmetric TE modes for digital ferrite phase shifters," *IEEE Trans. Microwave Theory Tech.*, vol. MTT-13, pp. 421-426, July 1965.
- [6] F. J. Bernues and D. M. Bolle, "A study of modes in circular waveguides loaded with azimuthally magnetized ferrite," Report NSF-GK 2351/1, Division of Engineering, Brown University, Apr. 1971.
- [7] R. E. Eaves and D. M. Bolle, "Perturbation theoretic calculation of differential phaseshifts in ferrite-loaded circularly cylindrical wave-

guides in the  $TE_{01}$  mode," *Electron. Lett.*, vol. 2, pp. 275-277, July 1966.

- [8] G. N. Tsandoulas and W. J. Ince, "Modal inversion in circular waveguides—Part I: Theory and phenomenology," *IEEE Trans. Microwave Theory Tech.*, vol. MTT-19, pp. 386-392, Apr. 1971.
- [9] G. N. Tsandoulas and W. J. Ince, "Modal inversion in circular waveguides—Part II: Application to latching nonreciprocal phasers," *IEEE Trans. Microwave Theory Tech.*, vol. MTT-19, pp. 393-401, Apr. 1971.
- [10] F. J. Bernues and D. M. Bolle, "The digital twin-ferrite toroid circular waveguide phaser," *IEEE Trans. Microwave Theory Tech.*, vol. MTT-21, pp. 842-845, Dec. 1973.
- [11] O. Parriaux and F. E. Gardiol, "Propagation of guided electromagnetic waves in symmetrical circularly cylindrical structures," *Wave Electronics*, vol. 1, pp. 363-380, June 1976.
- [12] C. L. Hogan, "The ferromagnetic Faraday effect at microwave frequencies and its applications," *Bell Syst. Tech. J.*, vol. 31, pp. 1-31, 1952.
- [13] C. R. Boyd, "A dual-mode latching reciprocal ferrite phase shifter," *IEEE Trans. Microwave Theory Tech.*, vol. MTT-18, pp. 1119-1124, Dec. 1970.
- [14] T. S. Chu, "Restoring the orthogonality of two polarizations in radio communication systems, I," *Bell Syst. Tech. J.*, vol. 50, pp. 3063-3069, Nov. 1971.
- [15] H. Kannowade, "Automatic compensation of cross-polarization coupling in communication systems using orthogonal polarizations," in *Problems of Space and Terrestrial Microwave Propagation*, Proc. Symp. European Space Agency, Graz, Austria, ESA SP 113, pp. 135-146, Apr. 1975.
- [16] J. L. Allen, "The analysis of ferrite phaseshifters including the effect of losses," Ph.D. dissertation, Georgia Institute of Technology, Atlanta, May 1966.
- [17] F. C. de Ronde, "Full waveguide band matching of waveguide discontinuities," *Proc. IEEE G-MTT Symp.*, 1967.

## Behavior of the Magnetostatic Wave in a Periodically Corrugated YIG Slab

MAKOTO TSUTSUMI, MEMBER, IEEE,  
YASUNORI SAKAGUCHI, AND NOBUAKI KUMAGAI,  
SENIOR MEMBER, IEEE

**Abstract**—An analysis for the propagation characteristics of the magnetostatic wave in a YIG slab having periodically corrugated surfaces is presented. The Brillouin diagrams, close to the intersection point  $(\omega, K)$  of  $m = 0$  and  $m = -1$  space harmonics, are obtained for different slab thicknesses, and the nonexistence of leaky wave modes has been established. Some discussions concerning the internal dc magnetic field and the propagation loss are also presented.

## I. INTRODUCTION

The periodic structures in dielectric media have long been a center of attraction of many researchers, particularly for their usefulness in many devices like filters, surface wave antennas, and distributed feedback (DFB) amplifiers in microwave and optical integrated circuits [1]–[4]. Recently, one of the present authors treated the case of propagation characteristics of magnetostatic waves in periodically magnetized ferrites where the internal dc magnetic field was modulated by providing additional magnets which were placed periodically around the YIG sample [5]. Also Elachi, in his paper [6], has studied the propagation of magnetic waves in an infinite periodic medium where he considered the dielectric constant of the medium to vary sinusoidally in space and treated the case of DFB-type magnetic wave oscillators. However, the effect of periodicity of the dielectric constant is rather small, because of the fact that a magnetic wave can propagate with no electric field components [7].

The present short paper investigates the propagation of the magnetostatic wave through a YIG slab having a periodically

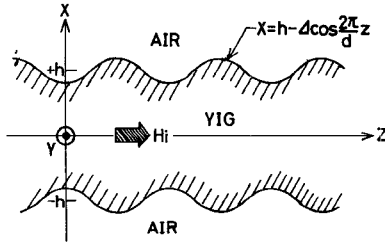


Fig. 1. Geometry of the corrugated structure.

corrugated surface. The Brillouin diagrams are obtained for the region close to the intersection point  $(\omega, K)$  of the fundamental mode of backward waves and the first space harmonic of forward waves. Some discussions are presented as regards the internal variation of the dc magnetic field and the associated propagation loss.

## II. DISPERSION RELATION

The geometry of the problem can be seen from Fig. 1. It consists of an open-guide structure and a periodically corrugated YIG slab with an average thickness of  $2h$  and a periodicity of  $d$ . Thus

$$x = h - \Delta \cos \frac{2\pi}{d} z \quad (1)$$

where  $\Delta$  is the strength of the modulation in the  $x$  direction. The biasing magnetic field  $H_i$  is assumed to be applied in the same direction as that of the magnetostatic wave propagation (i.e.,  $z$  direction). In the geometry of Fig. 1, the volume mode of the magnetostatic wave can propagate in accordance with the discussion in the paper of Damon and Eshbach [8].

The relation between the magnetic flux and the magnetic field in the medium can be expressed as

$$\mathbf{B} = \mu_0 \begin{pmatrix} \mu_1 & -j\mu_2 & 0 \\ j\mu_2 & \mu_1 & 0 \\ 0 & 0 & 1 \end{pmatrix} \cdot \mathbf{H} \quad (2)$$

assuming  $e^{-j\omega t}$  as the time dependence of the fields. In the preceding equation,  $\mu_1 = 1 + (\mu_0\gamma)^2 H_i M / ((\gamma\mu_0 H_i)^2 - \omega^2)$  and  $\mu_2 = \mu_0\gamma M \omega / ((\gamma\mu_0 H_i)^2 - \omega^2)$ ,  $\gamma$  being the gyromagnetic ratio and  $\mu_0 M$  the magnetic saturation.

In the quasi-static condition, Maxwell's equation can be approximated as

$$\nabla \times \mathbf{H} = 0 \quad (3)$$

and the RF magnetic field  $\mathbf{H}$  may be expressed in terms of the scalar magnetic potential  $\phi$  as

$$\mathbf{H} = -\nabla \phi. \quad (4)$$

By using (2), (4), and Gauss's law  $\nabla \cdot \mathbf{B} = 0$ , and further assuming the nondependence of the fields in the  $y$  direction, the magnetostatic potential equation may easily be obtained as

$$\mu_1 \frac{\partial^2 \phi}{\partial x^2} + \frac{\partial^2 \phi}{\partial z^2} = 0. \quad (5)$$

On the other hand, the magnetic potential  $\phi_0$  in air satisfies the relation

$$\frac{\partial^2 \phi_0}{\partial x^2} + \frac{\partial^2 \phi_0}{\partial z^2} = 0. \quad (6)$$

The proceeding analysis is carried out following the same analytical procedure as that of Dabby *et al.* [9] in a problem of the

propagation of electromagnetic waves in a periodic dielectric waveguide. However, this analytical method is based on a Rayleigh expansion which neglects the presence of incident waves in the corrugated region. Thus the solution obtained is more appropriate for the case of small modulations [3], [10]. The solutions of the magnetic potentials in air and YIG can conveniently be expressed in a similar form as the electric fields within a periodic dielectric waveguide

$$\phi_0 = \sum_{m=-\infty}^{+\infty} A_{m,p} e^{j(K_z + (2\pi/d)m)z} e^{-\gamma_m x - j\omega t} \quad (7)$$

and

$$\phi = \sum_{m=-\infty}^{+\infty} B_{m,p} \cos \left( K_{x,m} x - \frac{P}{2} \pi \right) e^{j(K_z + (2\pi m/d))z - j\omega t}. \quad (8)$$

In the preceding equations,  $A_{m,p}$  and  $B_{m,p}$  are the coefficients of space harmonics, and  $p$  denotes the mode pattern. Thus  $p = 1$  corresponds to the antisymmetric mode of the magnetic potential in the thickness direction and  $p = 2$  to the symmetric mode. Substituting (7) and (8) into (5) and (6), the transverse propagation constants  $\gamma_m$  and  $K_{x,m}$  can be related by

$$\gamma_m = \left| K_z + \frac{2\pi}{d} m \right| \quad (9)$$

and

$$K_{x,m} = \frac{1}{\sqrt{-\mu_1}} \left| K_z + \frac{2\pi}{d} m \right|. \quad (10)$$

The complete set of the expressions for the RF magnetic field components in YIG may be written from (2), (4), and (8) as

$$H_x = K_{x,m} \sin \left( K_{x,m} x - \frac{p\pi}{2} \right) G(z) B_{m,p} \quad (11)$$

$$H_z = -j \left( K_z + \frac{2\pi}{d} m \right) \cos \left( K_{x,m} x - \frac{p\pi}{2} \right) G(z) B_{m,p} \quad (12)$$

$$B_x = \mu_0 \mu_1 K_{x,m} \sin \left( K_{x,m} x - \frac{p}{2} \pi \right) G(z) B_{m,p} \quad (13)$$

and

$$B_z = -j \mu_0 \left( K_z + \frac{2\pi}{d} m \right) \cos \left( K_{x,m} x - \frac{p}{2} \pi \right) G(z) B_{m,p}. \quad (14)$$

In a similar fashion, the field components in the air region are written as

$$H_{x0} = \gamma_m e^{-\gamma_m x} G(z) A_{m,p} \quad (15)$$

$$H_{z0} = -j \left( K_z + \frac{2\pi}{d} m \right) e^{-\gamma_m x} G(z) A_{m,p} \quad (16)$$

$$B_{x0} = \mu_0 \gamma_m e^{-\gamma_m x} G(z) A_{m,p} \quad (17)$$

$$B_{z0} = -j \mu_0 \left( K_z + \frac{2\pi}{d} m \right) e^{-\gamma_m x} G(z) A_{m,p}. \quad (18)$$

In all the preceding expressions, the term  $G(z) = e^{j(K_z + (2\pi m/d))z - j\omega t}$ .

From the consideration of the periodic boundary conditions, the field components must be related to an extra term  $\theta$ , the gradients of the boundary surface due to the presence of the

corrugation, unlike in the case of a noncorrugated structure. The expression governing this is written as

$$\tan \theta = \frac{2\pi}{d} \Delta \sin \frac{2\pi}{d} z. \quad (19)$$

The application of the continuity condition for the tangential components of the RF magnetic field at  $x = h - \Delta \cos(2\pi/d)z$  results in

$$H_{z0} \cos \theta + H_{x0} \sin \theta = H_z \cos \theta + H_x \sin \theta \quad (20)$$

while the continuity of the normal components of the RF magnetic flux densities yields

$$B_{z0} \cos \theta + B_{x0} \sin \theta = B_z \cos \theta + B_x \sin \theta \quad (21)$$

where  $\tan \theta = \cot \theta$ . By substituting the field components of (11)–(18) into the boundary condition of (20), one can obtain

$$\begin{aligned} & \sum_{m=-\infty}^{+\infty} B_{m,p} \left\{ \left( K_z + \frac{2\pi}{d} m \right) \cos \left( K_{x,m} h - \frac{p\pi}{2} - \frac{|n-m|}{2} \pi \right) \right. \\ & \quad \cdot J_{|n-m|}(K_{x,m}\Delta) \\ & \quad + \frac{K_{x,m}}{d} \pi \Delta \left[ \sin \left( K_{x,m} h - \frac{p\pi}{2} - \frac{|n-m-1|}{2} \pi \right) \right. \\ & \quad \cdot J_{|n-m-1|}(K_{x,m}\Delta) \\ & \quad - \sin \left( K_{x,m} h - \frac{p\pi}{2} - \frac{|n-m+1|}{2} \pi \right) \\ & \quad \cdot J_{|n-m+1|}(K_{x,m}\Delta) \Big\} \\ & - \sum_{m=-\infty}^{+\infty} A_{m,p} e^{-\gamma_m h} \left\{ \left( K_z + \frac{2\pi}{d} m \right) I_{|n-m|}(\gamma_m \Delta) + \frac{\pi}{d} \Delta \gamma_m \right. \\ & \quad \cdot [I_{|n-m-1|}(\gamma_m \Delta) - I_{|n-m+1|}(\gamma_m \Delta)] \Big\} = 0. \quad (22) \end{aligned}$$

Also, the application of the boundary condition of (21) with the same set of field component's equations (11)–(18) yields

$$\begin{aligned} & \sum_{m=-\infty}^{+\infty} B_{m,p} \left\{ \mu_1 K_{x,m} \sin \left( K_{x,m} h - \frac{p\pi}{2} - \frac{|n-m|}{2} \pi \right) \right. \\ & \quad \cdot J_{|n-m|}(K_{x,m}\Delta) - \frac{\pi}{d} \Delta \left( K_z + \frac{2\pi}{d} m \right) \\ & \quad \cdot \left[ \cos \left( K_{x,m} h - \frac{p}{2} \pi - \frac{|n-m-1|}{2} \pi \right) \right. \\ & \quad \cdot J_{|n-m-1|}(K_{x,m}\Delta) \\ & \quad - \cos \left( K_{x,m} h - \frac{p}{2} \pi - \frac{|n-m+1|}{2} \pi \right) \\ & \quad \cdot J_{|n-m+1|}(K_{x,m}\Delta) \Big\} \\ & - \sum_{m=-\infty}^{+\infty} A_{m,p} e^{-\gamma_m h} \left\{ \gamma_m I_{|n-m|}(\gamma_m \Delta) - \left( K_z + \frac{2\pi}{d} m \right) \right. \\ & \quad \cdot \frac{\pi}{d} \Delta [I_{|n-m-1|}(\gamma_m \Delta) - I_{|n-m+1|}(\gamma_m \Delta)] \Big\} = 0. \quad (23) \end{aligned}$$

In the preceding equations,  $n$  is an integer with the limits of  $-\infty < n < +\infty$ , and  $J_n$  and  $I_n$  are the Bessel function and the modified Bessel function of the first kind, respectively. The above two equations of (22) and (23) are slightly more complex in form as compared to those of the periodic dielectric waveguide [9]. If this infinite set of homogeneous algebraic equations is to have a nontrivial solution, a determinant formed by the coefficients of  $A_{m,p}$  and  $B_{m,p}$  must vanish, leading to the final dispersion relation.

### III. NUMERICAL RESULTS

To obtain a numerical solution of the dispersion relation, the infinite set of homogeneous algebraic equations must be solved. The nature of the wave propagating through a periodic medium is that the  $m$ th harmonic gets coupled directly to the  $m-1$ th and  $m+1$ th harmonics and indirectly to the others [4]. Thus, neglecting the higher harmonics, the coupling region close to the intersection  $(\omega, K_z)$  of the  $m=0$  and  $m=-1$  space harmonics is important on the assumption that the modulation strength  $\Delta$  is very small, and further,

$$\begin{aligned} I_0(\gamma_m \Delta) & \simeq 1, \\ J_0(K_{x,m}\Delta) & \simeq 1, \\ I_n(\gamma_m \Delta) & \approx 0, \\ J_n(K_{x,m}\Delta) & \simeq 0, \quad n \neq 0. \end{aligned}$$

On these approximations, a simple dispersion relation may be obtained from (22) and (23) as

$$\begin{aligned} & \left\{ \sqrt{-\mu_1} \left[ 1 - \left( \frac{\pi}{d} \Delta \right)^2 \right] \cot S_{-1} - \left[ \mu_1 - \left( \frac{\pi}{d} \Delta \right)^2 \right] \right\} \\ & \quad \cdot \left\{ \sqrt{-\mu_1} \left[ 1 - \left( \frac{\pi}{d} \Delta \right)^2 \right] \cot S_0 - \left[ \mu_1 - \left( \frac{\pi}{d} \Delta \right)^2 \right] \right\} \\ & = \frac{- \left| K_z - \frac{2\pi}{d} \right|}{K_z - \frac{2\pi}{d}} \left( \frac{\pi}{d} \Delta \right)^2 (1 - \mu_1)^2 \quad (24) \end{aligned}$$

where

$$S_0 = \frac{1}{\sqrt{-\mu_1}} \left| K_z \right| h - \frac{p}{2} \pi \quad S_{-1} = \frac{1}{\sqrt{-\mu_1}} \left| K_z - \frac{2\pi}{d} \right| h - \frac{p}{2} \pi.$$

In the limiting case of  $\Delta = 0$  in (24), the coupling between the  $m=0$  and the  $m=-1$  space harmonic modes may be removed, leading to the following equations:

$$\sqrt{-\mu_1} \cot S_{-1} = \mu_1 \quad \sqrt{-\mu_1} \cot S_0 = \mu_1 \quad (25)$$

which are the ordinary dispersion relations of magnetostatic volume mode [8].

The typical Brillouin diagrams very near the coupling region are presented in Fig. 2 (a) and (b) for four different values of the modulation index  $\Delta/h$  and two different values of  $h/d$ , where the value of  $p$  is assumed to be unity. For the evaluation of (24), numerical values for the intensities of the internal magnetic field and the magnetic saturation are assumed to be  $5 \times 10^{-2}$  Wb/m<sup>2</sup> and  $1.73 \times 10^{-1}$  Wb/m<sup>2</sup>, respectively. The dispersion diagram for the volume mode of the  $m=0$  magnetostatic wave, in the frequency region limited between the resonance points of  $f_0 = 2.95$  GHz ( $f_0 = (\gamma\mu_0/2\pi)\sqrt{H_i(H_i + M)}$ ) and  $f_h = 1.41$  GHz ( $f_h = (\gamma\mu_0 H_i/2\pi)$ ), shows a negative group velocity characteristic in the absence of the corrugated surface [8]. On the other hand, a positive group velocity due to the  $m=-1$ th harmonic

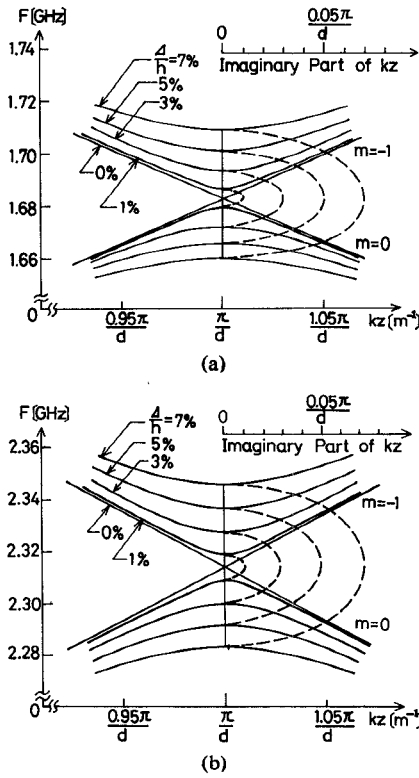


Fig. 2. Brillouin diagram very near the coupling region. —:  $K_z$  pure real. - - -:  $K_z$  complex. (a)  $h/d = 1$ . (b)  $h/d = 0.25$ .

mode appears in the presence of the surface corrugation, thus showing the existence of a coupling between the forward and the backward waves as shown in the solid lines of Fig. 2. Further, it can be seen that a stopband of range between 7 and 50 MHz appears if the  $\Delta/h$  value is changed from 1 to 7 percent as in Fig. 2 (a), whereas it is about 10 MHz in the case of  $\Delta/h = 1$  percent as in Fig. 2 (b). Thus the bandwidth can clearly be seen to be proportional to the magnitude of the modulation index  $\Delta/h$ . The comparison between Fig. 2 (a) and (b) indicates that the stopband width has a tendency to increase with decreasing values of  $h/d$ . The dashed line in Fig. 2 represents the complex value of the propagation constant within the stopband. This can be estimated numerically from the eigenvalue equation of (24) through some approximations such as

$$K_z = K_{z0} + \Delta K_z \quad \tan \frac{h}{\sqrt{-\mu_1}} \Delta K_z \simeq \frac{h}{\sqrt{-\mu_1}} \Delta K_z \quad (26)$$

where the propagation constant of  $K_{z0}$  satisfies the Bragg condition [4], i.e., by applying  $K_{z0} = \pi/d$ . Thus one obtains

$$\Delta K_z h = \sqrt{\frac{\left\{ \sqrt{-\mu_1} \left[ 1 - \left( \frac{\pi}{d} \Delta \right)^2 \right] \tan \left( \frac{1}{\sqrt{-\mu_1}} \frac{\pi}{d} h \right) + \left[ \mu_1 - \left( \frac{\pi}{d} \Delta \right)^2 \right] \right\}^2 - \left\{ \frac{\pi}{d} \Delta (1 - \mu_1) \right\}^2}{\left\{ \left[ \mu_1 - \left( \frac{\pi}{d} \Delta \right)^2 \right] \frac{1}{\sqrt{-\mu_1}} \tan \left( \frac{1}{\sqrt{-\mu_1}} \frac{\pi}{d} h \right) - \left[ 1 - \left( \frac{\pi}{d} \Delta \right)^2 \right] \right\}^2 - \left\{ \frac{1}{\sqrt{-\mu_1}} \frac{\pi}{d} \Delta (1 - \mu_1) \tan \left( \frac{1}{\sqrt{-\mu_1}} \frac{\pi}{d} h \right) \right\}^2}}. \quad (27)$$

When  $\tan((1/\sqrt{-\mu_1}) \cdot (\pi/d)h)$  within the root of (27) satisfies (25) and (26), (27) may be rewritten in the very simple form

$$\Delta K_z h = j \frac{\pi}{d} \Delta \quad (28)$$

which determines the maximum value of the purely imaginary  $\Delta K_z$ . Also, it can be seen from the dashed lines of Fig. 2 that the

value of  $\Delta K_z$  at Bragg frequency is about  $(0.05/d)\pi$  for  $\Delta/h = 5$  percent.

On the other hand, any leaky wave mode does not exist in the magnetostatic wave case unlike in the case of a periodic dielectric waveguide [2]. This is because of the simple fact that the transverse propagation constant in air is always real in any space harmonic, which can be interpreted as an evanescent mode.

Next, some general explanations of the present problem with regard to its utilities from practical design aspects are presented. The demagnetizing effects in the presence of corrugation are very important, especially for large indexes of modulation. The corrugated surface in fact enhances the variation of the internal dc magnetic field. In this case, the dispersion characteristics show the effects of both the corrugation and sinusoidal variation of the internal dc magnetic field [5]. However, the demagnetizing effect will be negligible in the case of small indexes of modulation and small periodicity, whereas the demagnetizing factor in magnetic field direction (i.e.,  $z$  direction), which appears in the presence of the finite length of slab, must be taken into account, particularly for a very thin YIG slab. Another factor is that it is practically slightly difficult to obtain a perfect corrugated surface by grooving mechanically the YIG surface, though the fundamental characteristic remains the same, as the corrugated shape is considered as one of the fundamental components of Fourier series expansion for the small indexes of the modulation.

The Brillouin diagrams are also shown for small thickness values of the slab. The propagation loss may be large for a very thin slab, since the transverse propagation constant  $K_x$  becomes small as is clear from (10) where  $|\mu_1|$  is nearly equal to 1 like Fig. 2 (b). This attributes to one practical limitation for filter applications; however, the loss may be reduced by using better materials [11]. Further, in the case of DFB-type magnetic oscillator applications, the frequency  $f$  should be chosen nearly equal to  $\gamma\mu_0 H_i/2\pi$ , (i.e.,  $|\mu_1| \gg 1$ ) as shown in Fig. 2 (a), [6], [12]. As a result, the loss in this frequency limit obviously carries much importance which must be given proper consideration.

#### IV. CONCLUSION

The preceding sections discussed the propagation problem of the magnetostatic wave in periodically corrugated surface of a YIG slab. The corresponding Brillouin diagrams have also been presented. Further, from the diagrams of the propagation constant within the stopband, a stopband frequency of about 10 MHz was obtained for a small modulation index of 1 percent. It has also been shown that no leaky mode exists at any frequency.

On the other hand, if we use the perturbation technique as has been discussed by Elachi *et al.* [13], the problems of a periodic structure considered here may be solved in a more simple form,

and also the perturbation technique may be versatile to solve complex problems like the propagation of magnetostatic surface waves in a corrugated YIG slab [11].

#### ACKNOWLEDGMENT

The authors wish to thank Dr. T. Bhattacharyya for his contributions to this work.

## REFERENCES

- [1] R. E. Collin, *Foundations of Microwave Engineering*. New York: McGraw-Hill, 1966, ch. 8, pp. 363-433.
- [2] A. A. Oliner and A. Hessel, "Guided-waves on sinusoidally-modulated reactance surfaces," *IRE Trans. Antennas Propagat.*, vol. AP-7, pp. 201-208, Dec. 1959.
- [3] S. T. Peng, T. Tamir, and H. Bertoni, "Theory of periodic waveguides," *IEEE Trans. Microwave Theory Tech.*, vol. MTT-23, pp. 123-133, Jan. 1975.
- [4] H. Kogelnik and C. V. Shank, "Coupled-wave theory of distributed feedback lasers," *J. Appl. Phys.*, vol. 43, pp. 2327-2335, May 1972.
- [5] M. Tsutsumi and Y. Yuki, "Magnetostatic wave propagation in a periodically magnetized ferrite," *J. Inst. Electron. Commun. Eng. Jap.*, vol. 58-B, pp. 16-23, Jan. 1975; in English, *Electronics & Communications in Japan*, vol. 58, s/p Scripta Pub. Comp. pp. 74-81, Jan. 1975.
- [6] C. Elachi, "Magnetic wave propagation in a periodic medium," *IEEE Trans. Magnetics*, vol. MAG-11, pp. 36-39, Jan. 1975.
- [7] Lax and Button, *Microwave Ferrites and Ferrimagnetics*. New York: McGraw-Hill, 1962, ch. 7, pp. 317-321.
- [8] R. W. Damon and J. R. Eshbach, "Magnetostatic modes of a ferromagnet slab," *J. Phys. Chem. Solids*, vol. 19, pp. 308-320, 1961.
- [9] F. W. Dabby, A. Kestenbaum, and U. C. Paek, "Periodic dielectric waveguides," *Opt. Commun.*, vol. 6, pp. 125-130, Oct. 1972.
- [10] M. Neviere, R. Petit, and M. Cadilhac, "About the theory of optical grating coupler-waveguide systems," *Opt. Commun.*, vol. 8, pp. 113-117, June 1973.
- [11] J. D. Adam and J. H. Collins, "Microwave magnetostatic delay devices based on epitaxial yttrium iron garnet," *Proc. IEEE*, vol. 64, pp. 794-800, May 1976.
- [12] B. Vural, "Interaction of spin waves with drifted carriers in solids," *J. Appl. Phys.*, vol. 37, pp. 1030-1031, Mar. 1966.
- [13] C. Elachi and C. Yeh, "Mode conversion in periodically distributed thin film waveguides," *J. Appl. Phys.*, vol. 45, pp. 3494-3499, Aug. 1974.

## On the Theory and Application of the Dielectric Post Resonator

MARIAN W. POSPIESZALSKI

**Abstract**—This short paper deals with the modes of the dielectric post resonator when  $\epsilon_r$  is large. The normalized frequency  $F_0 = (\pi D/\lambda_0) \sqrt{\epsilon_r}$  as a function of  $D/L$  is discussed. The simple approximate expressions for the resonant frequencies of the lower order modes are given. The properties of the  $TE_{011}$  mode are discussed in detail from the point of view of its application to the measurement of the complex permittivity of microwave dielectrics. Curves and expressions for fast and simple determination of the maximum measurement errors are given.

## I. INTRODUCTION

In this short paper, the resonant properties of the structure shown schematically in Fig. 1 will be discussed. The cylindrical sample of a low-loss high- $\epsilon_r$  dielectric material is placed between two parallel conducting plates. This structure, known in the literature as the dielectric post resonator, was applied by Hakki and Coleman [1], and later by Courtney [2], to measurements of the complex permittivity and complex permeability of microwave insulators. It was also used to provide high RF field concentrations on ferrite crystals [3], [5]. Present availability of the low-loss high- $\epsilon_r$  temperature compensated ceramics (for instance, [6], [7]) should permit introduction of this structure as an element of microwave filters, oscillators, etc. Information on the modes of the dielectric post resonator that can be found in the literature are valid only for certain values of  $\epsilon_r$  [2]-[4]. A mode chart, together with approximate expressions for the resonant frequencies of the lower order modes, valid for all cases when  $\epsilon_r \geq 10$  is given. Though the properties of the

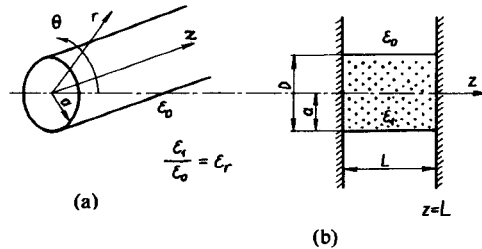


Fig. 1. Dielectric rod placed between two infinite parallel perfectly conducting plates.

particular  $TE_{011}$  mode were discussed in detail [1], [2], some important simplifications can be carried out, as is shown in the following.

## II. DIELECTRIC POST RESONATOR

## Basic Relations

Referring to Fig. 1, the dielectric post resonator can be described as a dielectric rod transmission line short circuited at both ends. The characteristic equation for the normal modes of the structure [8], [9] can be written in the form

$$(J^+ + K^+) \left( J^- - \frac{K^-}{\epsilon_r} \right) + (J^- - K^-) \left( J^+ + \frac{K^+}{\epsilon_r} \right) = 0 \quad (1)$$

$$\left( \frac{\pi D}{\lambda_0} \right)^2 \epsilon_r = u^2 + \left( \frac{\pi D l}{2L} \right)^2 \quad (2)$$

$$w^2 = \left( \frac{\pi D l}{2L} \right)^2 - \left( \frac{\pi D}{\lambda_0} \right)^2 \quad (3)$$

and

$$J^- = \frac{J_{n-1}(u)}{u J_n(u)} \quad J^+ = \frac{J_{n+1}(u)}{u J_n(u)} \\ K^- = \frac{K_{n-1}(w)}{w K_n(w)} \quad K^+ = \frac{K_{n+1}(w)}{w K_n(w)}$$

where  $J_n$  is the Bessel function of the first kind of  $n$ th order,  $K_n$  is the modified Hankel function of  $n$ th order,  $l$  is the number of half-wavelengths in the cavity along the axial direction,  $D$  and  $L$  are the diameter and length, respectively,  $\epsilon_r$  is the relative dielectric constant, and  $\lambda_0$  is the free-space wavelength corresponding to the resonant frequency  $f_0$ . The solution of the preceding set of equations can be most conveniently presented in the form  $F_0^2 = (\pi D/\lambda_0)^2 \epsilon_r = f_1(D/L)$ .  $F_0$ , which we call a normalized frequency variable, is very small dependent on  $\epsilon_r$  when  $\epsilon_r$  is much greater than unity. Indeed, for all values  $D/L > 0$  and  $\epsilon_r \rightarrow \infty$ , the asymptotic form of the previous equations is

$$(J^+ + K^+) J^- + (J^- - K^-) J^+ = 0 \quad (4)$$

$$F_0^2 = u^2 + w^2 \quad (5)$$

$$w = \frac{\pi D l}{2L} \quad (6)$$

This is very well illustrated by the mode chart for the lower order modes shown in Fig. 2. The solutions for  $\epsilon_r \geq 500$  cannot be distinguished graphically. The largest difference in the range of interest for these cases is 0.46 percent for the  $TE_{011}$  mode and  $(D/L)^2 = 0.5$ .